Acta Physicae Superficierum · Vol II · 1990

ANGULAR DISTRIBUTION OF PLANAR CHANNELED PROTONS IN Si CRYSTAL*

JERZY CZERBNIAK

Institute of Physics, University of Łódź
M. Nowotki 149/153, 90-236 Łódź, Poland

ABSTRACT. Measurements of the planar channeling of 50, 100, 150 keV protons in Si, for a variety of atomic planes are presented. The observed half-angles at half minimum $\varphi_{1/2}$ and minimum yield χ_{min} are compared with the theoretical ones calculated by solving the equation of ion movement between the planes.

INTRODUCTION

The channeling phenomenon in connection with random backscattering technique (RBS) provides a very useful tool for applications in crystal physics [1–3]. At commonly used ion energies of 1 MeV, the surface impurities and defects exert small influence on the channeling process. In the case of lower energy range i.e. 100 keV and light ions, the contaminations and structure defects of the surface have to be considered. Perturbation of channeled ion movement can be caused at the surface, during the entrance to the channel, and then during the channeling in the bulk.

Descriptions of ion movement trajectory are based on the concept of an averaged potential of ion crystal/axis interaction [4–5]. The characteristic parameters of channeling ($\varphi_{1/2}$, χ_{min}) obtained in this model are in good agreement with experimental results, particularly in the higher ion energy range. Similar results can be obtained by application of Monte Carlo methods to channeling [6–8]. In this approach all the factors of ion movement perturbance at the surface (structure defects and amorphous surface layers) can be included into calculation as well as experimental conditions, such as energy and angle distributions of the initial ion beam, enabling a satisfactory interpretation of experimental data. The immediate results obtained in experiment are the energy distributions of backscattered ions recorded at different angles of ion incidence in the channel, determined with respect to the crystal plane or axis.

* The work was partly supported by CPBP 01.08.

In the low energy range measurement of the RBS spectrum requires the use of an electrostatic analyser, and this extends the measurement time interval so considerably as to cause additional radiation damage. Some of channeling characteristics can be obtained directly by measurements of the average value of scattering cross-section, averaged over the depth $0-x$ (Fig. 1).

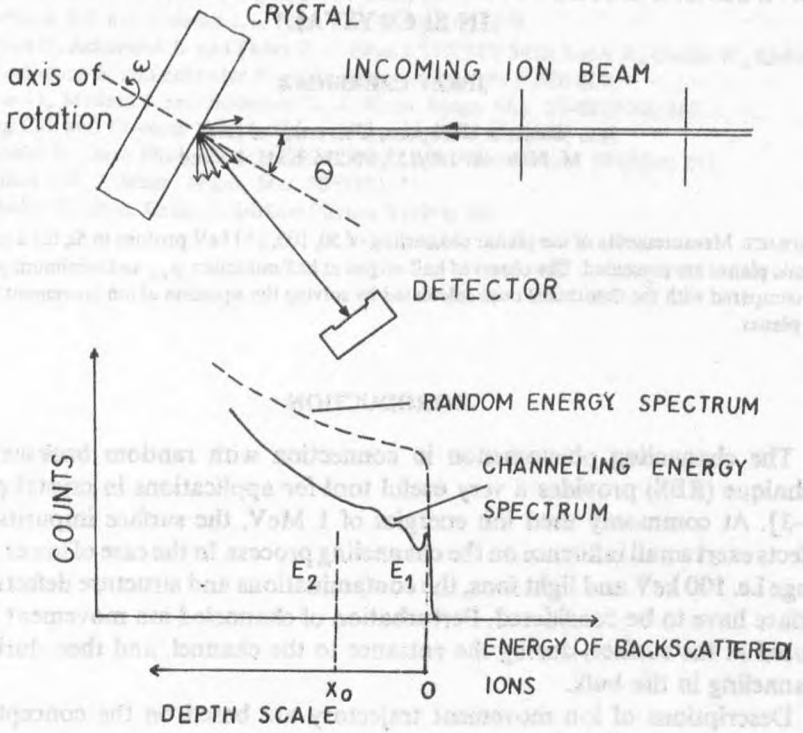

Fig. 1. Schematic diagram of the experimental arrangement.

DESCRIPTION OF THE EXPERIMENTAL SETUP

Protons produced in the high frequency ion source were sped up in a linear accelerator up to an energy of 200 keV. The ion flux was collimated with diaphragms of diameter down to 1.5 mm providing 0.04 deg of angular divergence. The initial ion energy was determined with 4% accuracy. The investigated single crystal was mounted on a two-axis goniometer, with 0.05 deg of angle resolution. The backscattered protons were detected by a surface barrier detector. The conditions of measurement were chosen so as to record protons

backscattered from a penetration depth of 0–150 nm. The maximum irradiation dose was kept below 10^{14} ion/cm^2. The crystal was cut perpendicularly to its ⟨111⟩ axis, and the surface was prepared directly before each measurement; after cleaning in an alcohol mixture (96% ethyl and 4% methyl alcohol) the crystal was oxidated in a temperature of 1100 K and steam, then SiO_2 on the surface, was etched in HF acid, and immediately after cleaning in ethanol the crystal was introduced into the vacuum reaction chamber. The geometry of experiment is presented in Fig. 1. A detailed analysis of the positions of angular RBS minima enabled us to determine precisely the actual values of the tilt angle θ and the actual rotation axis (see Appendix). The declination is caused mainly by the cut of the crystal. For the commonly used Si crystal samples it approached ∓ 1 deg. The worked-out procedure of determination of the rotation axis and angle θ is charged with an error of less than 0.01 deg. A typical example of the angular spectrum is depicted in Fig. 2a.

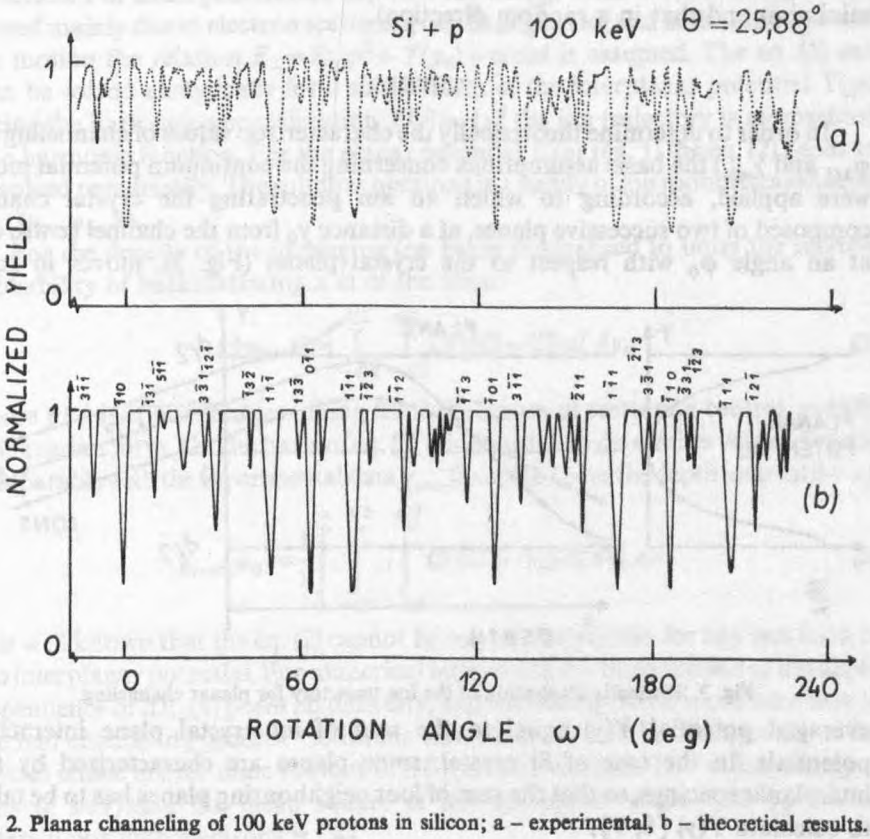

Fig. 2. Planar channeling of 100 keV protons in silicon; a – experimental, b – theoretical results.

The main difficulty encountered when interpreting the spectra is the establishing of direct correspondence between the observed RBS minima and the crystal planes in which the channeling process takes place. Due to the widths of channeling dips overlaps of neighbouring minima can be observed, the greater the lower is the ion energy and the smaller the tilt angle θ. In order to overcome the difficulties, a computer code was written, which let us determine theoretically the expected positions of the minima taking into account channeling in low and medium index crystallographic planes. As input parameters of the code were chosen: charge and energy of the ion, the type of crystal, the tilt angle θ, the arrangement of the crystal and rotation axis and the function describing the dependence between maximum width of dip and the type of crystallographic plane. The output of the procedure, the RBS angle spectrum, schematically plotted in Fig. 2b, enabled us to determine unambiguously all the minima which are the result of planar channeling of the ion along one crystallographic plane. Only for these dips was it possible to estimate $\varphi_{1/2}$ (the half-width at the half-minimum) and χ_{min} (minimum yield – the ratio of counts number in the minimum and that in a random direction).

THEORY

In order to determine theoretically the characteristic values of channeling (i.e. $\varphi_{1/2}$ and χ_{min}) the basic assumptions concerning the continuum potential model were applied, according to which an ion penetrating the crystal channel composed of two successive planes, at a distance y_0 from the channel centre and at an angle φ_0 with respect to the crystal planes (Fig. 3), moves in some

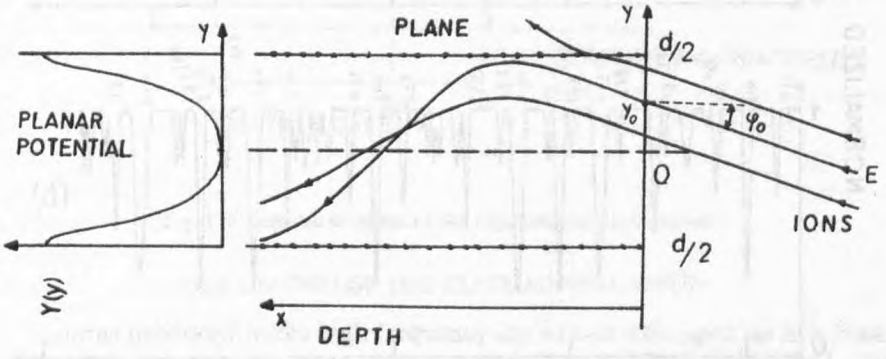

Fig. 3. Schematic illustration of the ion trajectory for planar channeling.

averaged potential $Y(y)$ equal to the sum of ion-crystal plane interaction potentials. In the case of Si crystal, some planes are characterized by two interplanar spacings, so that the sum of four neighbouring planes has to be taken to calculate $Y(y)$ [8, 9]:

$$Y(y)=\sum_{i=1}^{4} U_i(y), \qquad y=d/2-z$$
$$U(z)=2\pi Z_1 Z_2 e^2 N d\left[(z^2+\rho_\perp^2+a_{TF}^2)^{1/2}-(z^2+\rho_\perp^2)^{1/2}\right] \tag{1}$$

where Z_1 and Z_2 are the atomic numbers of the projectile and substrate atoms, respectively, N is the density of substrate atoms, d the interplanar spacing, a_{TF} the Thomas-Fermi screening distance, $\rho_\perp^2$ the mean square of thermal vibration amplitude, and z the distance from the plane. The equation of ion motion between two planes is:

$$\frac{m}{2}\left(\frac{dy}{dt}\right)^2+Y(y)=E_0\varphi_0^2+Y(y_0)+\Delta E_\perp(x) \tag{2}$$

where the left-hand side of the equation describes the sum of potential and kinetic energy in the one-dimensional ion motion across the channel, and the right-hand side is the total energy of transverse ion motion, generally dependent on the path traversed. For small penetration depths x the change in transverse energy $\Delta E(x)$ caused mainly due to electron scattering can be neglected, and in the initial part of ion motion the relation $E_\perp=E_0\varphi^2+Y(y_0)=\text{const}$ is assumed. The eq. (3) can then be solved analytically for a simple form of the interplanar potential $Y(y)$; taking the harmonic approximation $Y(y)=Ay^2$ the ion trajectory is represented by a harmonic function. For the planar potential $U(y)$ (eq. 1) the eq. (2) needs to be solved numerically. The solution obtained is a family of ion motion trajectories $\zeta=f(y_0, \varphi_0, x)$.

For the density of the impinging ion beam normalized to unity the relative probability of backscattering x is of the form:

$$\chi(\varphi_0, x)=\int_{-d/2}^{d/2}\int_{-d/2}^{d/2}\zeta p(d/2-|\zeta|)\,d\zeta\,dy_0 \tag{3}$$

where $p(\cdot)$ is a function describing the distribution of scattering centres, usually of Gaussian form. On the basis of eq. (3) it is possible to determine values directly comparable with the experimental data χ_{aver} (averaged over the depth interval $0-x$):

$$\chi_{aver}(\varphi_0)=\frac{1}{x}\int_0^x\int_{-d/2}^{d/2}\int_{-d/2}^{d/2}\zeta p(d/2-|\zeta|)\,d\zeta\,dy_0\,dx. \tag{4}$$

It is well known that the eq. (2) cannot be solved analytically for any real form of the interplanar potential. For numerical integration the introduction of the depth dependence of $\Delta E_\perp(x)$ poses no difficulty, and the description is more adequate to the real channeling process. Collisions with electrons and inhomogeneity of the crystal lattice are the main reasons of $\Delta E_\perp(x)$ enhancement. For an ion energy of tens of keV/amu the mean square of the fluctuation angle $\langle\Delta\Omega^2\rangle_e$ due to interactions with electrons is [4]:

$$\langle \Delta\Omega^2 \rangle_e = (m_e/2M_1 E)(-dE/dx)\,\Delta x$$
$$\Delta E_\perp(x) = E\langle \Delta\Omega^2 \rangle_e \tag{5}$$

where m_e is the electron mass and $(-dE/dx)$ the stopping power. Performing the calculations of $\chi_{aver}(\varphi_0)$ (eqs. 2, 4 and 5) for different angles of incidence φ_0 the full shape of the dip can be obtained and, in this way, the theoretical values of χ_{min} and $\varphi_{1/2}$ can be compared immediately with experiment.

ANALYSIS OF THE EXPERIMENTAL RESULTS

The results obtained directly in experiment are the angle distributions of backscattered ions (Fig. 3) measured for different energies and crystal inclination angles. On the basis of several tens of angle distributions, the shape of the dips corresponding to proton channeling along the main Si crystal

TABLE 1
Half-angles and minimum yield for planar channeling of proton in Si crystal.

Energy		50 keV		100 keV		150 keV	
Plane		exper.	theor.	exper.	theor.	exper.	theor.
{113}	$\varphi_{1/2}$	0.52(4)	0.55	0.35(3)	0.39	0.31(2)	0.32
	χ_{min}	0.75(4)	0.70	0.73(4)	0.68	0.73(4)	0.68
{112}		0.53(3)	0.56(4)	0.36(3)	0.39	0.29(2)	0.31
		0.74(4)	0.68	0.74(4)	0.66	0.72(4)	0.66
{110}		0.74(2)	0.84	0.54(2)	0.60	0.44(2)	0.48
		0.44(2)	0.41	0.35(2)	0.32	0.35(2)	0.31

planes (110), (112), (113) was approximated and the values of χ_{min} and $\varphi_{1/2}$ determined (Table 1). A comparison of the theoretical and experimental angular dips is given in Fig. 4 for 100 keV energy protons and the (110) Si plane. The theoretically determined values of $\varphi_{1/2}$ are by several per cent larger than those measured, suggesting that the height of the potential barrier is decreased in comparison with that obtained from eq. (1). Experiments performed at higher energies (above 0.2 MeV) [10] yield very good agreement with the theoretical values of $\varphi_{1/2}$, proving that the Lindhard potential correctly describes the channeling process under these conditions. The $\varphi_{1/2}$ values were determined using χ_{min} and χ_{rand}, meaning that any change in either the former or the latter value strongly affects $\varphi_{1/2}$. By 'any change' there may be understood all the factors which cannot be taken into account solving eq. (2) and which occur in real experimental conditions. Here belong the energy dependent angle dispersion of the ion beam caused by the finite accuracy of ion beam collimation and the

additional dispersion at the crystal surface. From the classical theory of scattering it is known that the averaged square of the multiple scattering angle due to scattering on the nuclei is:

$$(\Omega^2)_n = \frac{2\pi Z_1^2 Z_2^2 e^4 N L_n}{E^2}\,\Delta x \qquad (6)$$

$$L_n = \ln 1.29\,\frac{a_{TF} M_2 E}{Z_1 Z_2 e^2 (M_1 + M_2)}.$$

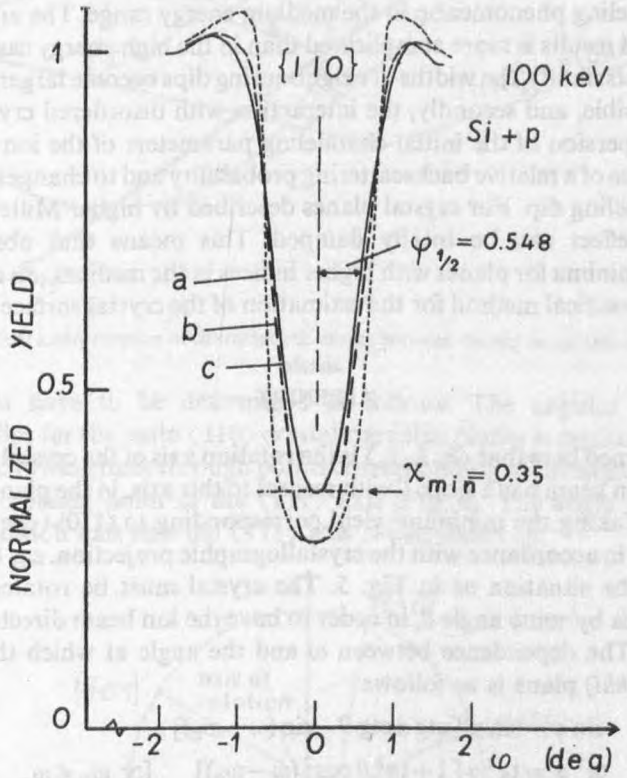

Fig. 4. Scattering yield of protons channeled along the {110} Si plane; a – calculation without surface multiple scattering, b – calculation including multiple scattering, c – experimental results.

In the high energy range the latter factor plays no role; for low energies, however, it becomes important, meaning that the ions entering the channel have no unambiguously defined angle of incidence φ_0. Assuming that the dispersion of the incidence angle caused by interaction with a disordered crystal surface can be described by a Gaussian distribution, with the standard deviation calculated according to eq. (6), the shape of the minimum is obtained (using eq. 4) as:

$$\chi_{\text{real}}(\varphi_0) = \int_{-\infty}^{+\infty} \chi_{\text{aver}}(\varphi_0)\, p(\varphi_0)\, d\varphi_0 . \tag{7}$$

The dip after such a transformation is plotted in Fig. 4, and it is evident that the χ_{real} values satisfactorily describe the experimental values of χ_{min} and the shape of the dip.

CONCLUSIONS

The averaged, continuous potential model permits a satisfactory description of the channeling phenomenon in the medium energy range. The analysis of the experimental results is more complicated than in the high energy case, due to the following facts: firstly, the widths of neighbouring dips become larger, making dip overlap possible, and secondly, the interaction with disordered crystal surfaces causes a dispersion of the initial channeling parameters of the ion beam. Both lead to the rise of a relative backscattering probability and to changes in the shape of the channeling dip. For crystal planes described by higher Miller indices the channeling effect can be totally damped. This means that observation of channeling minima for planes with higher indices in the medium ion energy range provides a practical method for the estimation of the crystal surface parameters.

APPENDIX

It is assumed here that $\langle h_0 k_0 l_0 \rangle$ is the rotation axis of the crystal and that the impinging ion beam has a slope θ with respect to this axis, in the plane containing both lines. Taking the minimum yield corresponding to (110)-type planes, and describing it in accordance with the crystallographic projection, e.g. $(1\bar{1}0)$, we are faced with the situation as in Fig. 5. The crystal must be rotated about the $\langle h_0 k_0 l_0 \rangle$ axis by some angle θ, in order to have the ion beam directed along the (hkl) plane. The dependence between ω and the angle at which the ion beam crosses the (hkl) plane is as follows:

$$\begin{aligned} &\sin\varphi = \sin\alpha'[\operatorname{ctg}\alpha \operatorname{ctg}\theta - \sin(\omega-\omega_0)], \\ &\operatorname{tg}^2\alpha' = \operatorname{tg}^2\alpha[1+\operatorname{tg}^2\theta\cos^2(\omega-\omega_0)] \quad \text{for } \omega_0<\omega, \\ &\operatorname{tg}^2\alpha' = \operatorname{ctg}^2\omega + \operatorname{ctg}^2\theta/\sin^2(\omega-\omega_0) \quad \text{for } \omega_0>\omega. \end{aligned} \tag{I}$$

In experiment the $\omega_{1/2}$ angles are measured, and using (I) the values of $\varphi_{1/2}$ can be calculated:

$$\begin{aligned} &\varphi_{1/2} = \omega_{1/2}\sin\alpha'\sin\theta\cos(\omega_{\text{min}}-\omega_0), \\ &\sin(\omega_{\text{min}}-\omega_0) = \operatorname{ctg}\alpha\operatorname{ctg}\theta . \end{aligned} \tag{II}$$

Assuming that $\langle 111 \rangle$ is the rotation axis, the value of α is known. When the actual rotation axis creates a $\Delta\alpha$ angle with the $\langle 111 \rangle$ axis, the indices h_0, k_0, l_0 of the

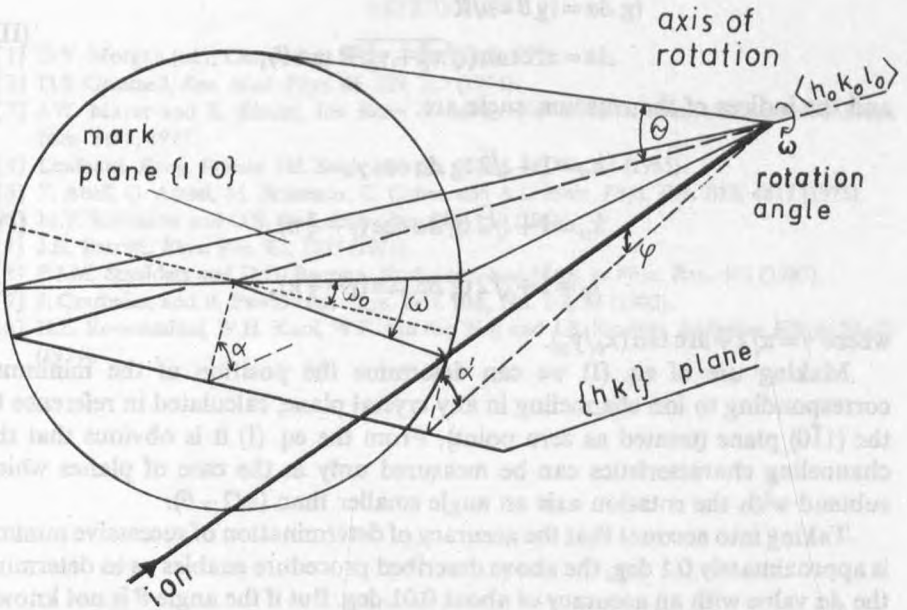

Fig. 5. Geometrical interpretation of characteristic angles between the ion beam and crystallographic planes.

rotation axis have to be determined as follows. The angular position of channeling dips for the main ⟨110⟩ crystallographic planes is marked on a circle of radius R. Drawing lines through points corresponding to the same planes, one obtains the crossing point of the ⟨111⟩ axis (Fig. 6). The angle between the $\langle h_0 k_0 l_0 \rangle$ rotation axis and the ⟨111⟩ axis is calculated as:

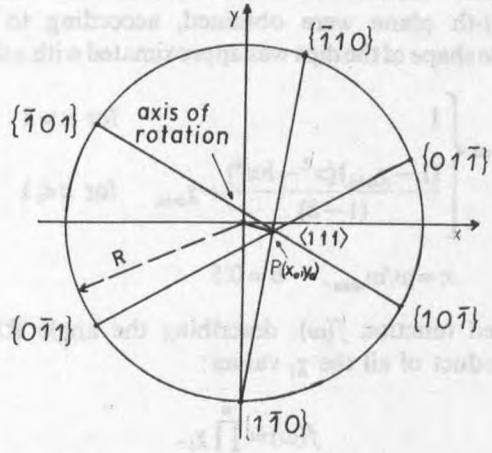

Fig. 6. Schematic stereographic representation of Si crystal rotation about the $\langle h_0 k_0 l_0 \rangle$ axis.

$$\operatorname{tg}\Delta\alpha = \operatorname{tg}\theta * a/R$$
$$\Delta\alpha = \arctan\left(\sqrt{x_0^2 + y_0^2}/R \tan\theta\right), \tag{III}$$

and the indices of the rotation angle are:

$$h_0 = 1 + \sqrt{2}\operatorname{tg}\Delta\alpha\cos\gamma,$$
$$k_0 = 1 + \sqrt{2}\operatorname{tg}\Delta\alpha\cos\left(\gamma - \tfrac{2}{3}\pi\right), \tag{IV}$$
$$l_0 = 1 + \sqrt{2}\operatorname{tg}\Delta\alpha\cos\left(\gamma - \tfrac{4}{3}\pi\right),$$

where $\gamma = \pi/2 + \arctan(x_0/y_0)$.

Making use of eq. (I) we can determine the position of the minimum corresponding to ion channeling in any crystal plane, calculated in reference to the $(1\bar{1}0)$ plane (treated as zero point). From the eq. (I) it is obvious that the channeling characteristics can be measured only in the case of planes which subtend with the rotation axis an angle smaller than $(\pi/2 - \theta)$.

Taking into account that the accuracy of determination of successive minima is approximately 0.1 deg, the above described procedure enables us to determine the $\Delta\alpha$ value with an accuracy of about 0.01 deg. But if the angle θ is not known exactly enough, the above described procedure can be applied for other types of planes, for example (113) and (112) types, to determine the actual θ and $\Delta\alpha$ angles by the multidimensional regression method, with accuracy of an order better than the precision of the goniometer.

The theoretical RBS angle spectra were determined as follows: the position of the i-th plane was established, the theoretical values of $\varphi_{\max}$ corresponding to the height of the potential barrier were calculated from the relation $E\varphi_{\max}^2 = Y(d/2)$, using eq. (I) the values were calculated, the theoretical values of χ_{theor} for the i-th plane were obtained, according to [4, 9] as $\chi_{\text{theor}} = 2(a_{\text{TF}} + \rho_\perp)/d_i$; the shape of the dips was approximated with a simple polynomial:

$$\chi_i = \begin{cases} 1 & \text{for } x > 1 \\ \dfrac{(1-\chi_{\min})(x^2 - bx^4)}{(1-b)} + \chi_{\min} & \text{for } x \leqslant 1 \end{cases}$$

$$x = \omega/\omega_{\max}, \qquad b = 0.5$$

and the normalized function $f(\omega)$, describing the angle RBS spectrum was calculated as a product of all the χ_i values:

$$f(\omega) = \prod_{i=1}^{n} \chi_i.$$

REFERENCES

[1] D.V. Morgan (ed.), *Channeling*, Wiley, New York, 1973.
[2] D.S. Gemmell, *Rev. Mod. Phys.* **46**, 129, 217 (1974).
[3] J.W. Mayer and E. Rimini, *Ion Beam Handbook for Material Analysis*, Academic Press, New York, 1977.
[4] Lindhard, *Kong. Danske Vid. Selsk., mat-fys. Medd.* **34**, No. 14 (1965).
[5] F. Abell, G. Amsel, M. Bruneaux, C. Cohen and A.L. Hoir, *Phys. Rev.* **B12**, 4617 (1975).
[6] M.T. Robinson and O.S. Oen, *Phys. Rev.* **166**, 219 (1968).
[7] J.H. Barrett, *Phys. Rev.* **B3**, 1527 (1971).
[8] P.J.M. Smulders and D.O. Boerma, *Nucl. Instr. and Meth. in Phys. Res.*, 471 (1987).
[9] J. Czerbniak and B. Pawłowski, Phys. Lett. **90A**, No. 1-2, 65 (1982).
[10] H.E. Rooseendaal, W.H. Kool, W.F. van der Weg and J.B. Sanders, *Radiation Effects* **22**, 22 (1974).